International Journal of Engineering

Journal Homepage: www.ije.ir

RESEARCH NOTE

Structure-property Interaction in Flux Assisted Tungsten Inert Gas Welding of Austenitic Stainless Steel

G. Singh*, D. Kumar Shukla

Department of Mechanical Engineering, Dr. B.R. Ambedkar National Institute of Technology, Jalandhar, Punjab, India

P A P E R I N F O

Paper history:
Received 11 May 2018
Received in revised form 03 Januray 2019
Accepted 03 Januray 2019

Keywords:
Active Tungsten Inert Gas
Marangoni Convection
Mechanical Properties
Austenitic Stainless Steel

A B S T R A C T

Austenitic stainless steel SS304 grade was welded with active Tungsten Inert Gas (TIG) welding process by applying a flux paste made of SiO_2 powder and acetone. SiO2 flux application improves the weld bead depth with a simultaneous reduction in weld bead width. The improvement in penetration results from arc constriction and reversal of Marangoni convection. Experimental studies revealed that the SiO_2 flux assisted TIG welding can enhance the weld bead penetration by more than 100%. Full depth welds up to 6mm were obtained by applying SiO_2 flux. Microstructure reveals a reduction in ferrite formation in fusion zone by applying SiO_2 flux. Samples welded with flux exhibits reduction in tensile strength and improvement in impact strength. Fractography of the tensile test specimens reveals the presence of oxide inclusions in the samples welded with flux. The relation of ferrite content and mechanical properties are presented in this paper.

***doi**: 10.5829/ije.2019.32.01a.13*

1. INTRODUCTION

Tungsten Inert Gas (TIG) Welding Process or Gas Tungsten arc welding (GTAW) process uses a non-consumable tungsten electrode to generate an electric arc for fusion of work-piece. The electrode is protected with inert gas generally argon or helium to prevent oxidation at high temperature. This process is commonly used for good quality welds of stainless steel, alloy steels, magnesium and aluminum alloys [1]. However, the process lacks in achieving penetration greater than 3mm. Full depth fusion joints are made by V-Groove edge preparations and multi-pass welding procedures which reduce the productivity of process [2]. There was a definite need to improve the weld bead penetration in GTAW process.

Several techniques have been implemented in past to improve the weld bead penetration. Heiple et al. [3] proposed theories that change in the surface tension driven flow of the molten metal in weld pool can remarkably improve the weld bead geometry. Some of the alloying elements like sulfur, selenium can act as a surface active agent in the weld pool to change the surface tension driven flow. This can additionally enhance the weld penetration and depth/width proportion of the weld bead. Whereas some elements like phosphorus have not shown any effect on the weld bead geometry [4]. It was in this manner inferred that exclusive surface dynamic components like sulfur, selenium, oxygen over a specific point of confinement can change the surface strain driven stream to enhance the GTAW Productivity. In another technique, developed by Paton Institute of welding in the 1960s, active flux powder containing oxides, chlorides are applied to the base material before welding [5]. This technique gained the interest of researchers from the year 2000 onwards to improve weld bead geometry [6]. In this technique, active flux made of oxide powders is blended with a thinner like acetone or ethanol to have a paint-like consistency. It is applied to the base metal before welding as shown in Figure 1. At high temperature during welding, oxygen decomposes from the oxide powders [7]. Oxygen being a surface active element reverses the Marangoni flow to improve weld bead geometry [8]. Whereas some of the researchers consider arc constriction for improvement of weld bead penetration [9].

*Corresponding Author Email: *gurveensingh03@gmail.com* (G. Singh)

Please cite this article as: G. Singh, D. K. Shukla, Structure-property Interaction in Flux Assisted Tungsten Inert Gas Welding of Austenitic Stainless Steel, International Journal of Engineering (IJE), IJE TRANSACTIONS A: Basics Vol. 31, No. 1, (January 2019) 99-105

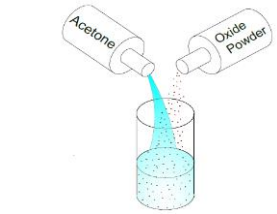

(a) Blending

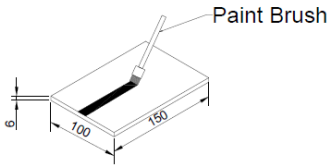

(b) Applying

Figure 1. Application of Active flux [10]

The process is generally known as Active TIG Welding Process (A-TIG). Silicon dioxide (SiO_2) has been used in past by some researchers and it was observed to be the most effective oxide powder for preparation of active flux. The goal of present study was to explore the impact of SiO_2 flux on weld bead microstructure and mechanical properties of weld joint and present the inter-relationship of microstructure and mechanical behavior.

1. 1. Mechanisms of Penetration Improvement

Two mechanisms viz Marangoni convection and arc constriction are most usually acknowledged for clarifying the change of penetration in flux assisted GTAW process. Marangoni convection states that fluid flow is controlled by surface tension gradient. Fluid flows from the region of lower surface tension to the region of higher surface tension [11]. Oxygen decomposes from the oxide powders at high temperature and being a surface active element for ferrous materials, it changes the surface tension driven flow [12]. Initially, the surface tension was higher at the edge of the weld pool and lower at the center. With the presence of oxygen in the weld pool, the surface tension gradient of the weld pool reverses and surface tension becomes higher at center and lower at the edge of weld pool [13, 14]. This reversal of surface tension flows the liquid metal down rather than outward flow as depicted in Figure 2. Many researchers had used this phenomenon to explain the improvement in penetration obtained by use of active flux powders [15, 16].

Some of the researchers captured images of arc during welding with and without active flux. They observed constriction in weld arc when active flux was used in welding [17]. Arc constriction was attributed to the electronegativity of ions of the active element present in weld pool [18]. When weld pool contains sufficient amount of active element, the arc column diameter reduces thereby increasing the heat density or the anode root area thus leading to enhancement of weld penetration.

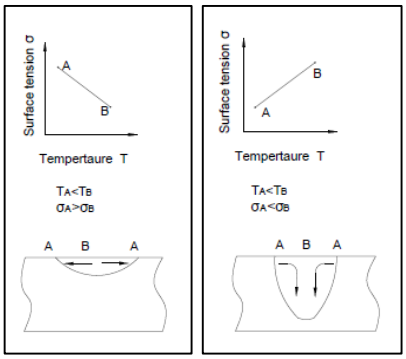

(a) (b)

Figure 2. Marangoni Flow: (a) Without Active Flux (b) With Active Flux [2]

2. EXPERIMENTATION

A direct current power source (EWM-Tetrix 351) with electrode negative polarity was used with an automated system by which the specimen was moved at a consistent speed while keeping the torch fixed. A water-cooled torch with 2% thoriated tungsten electrode of diameter 2.4 mm was used in this study. Electrode vertex angle of 30^0, Electrode to workpiece distance of 2mm and electrode extension of 3 mm was kept fixed for all experiments. Argon was selected as the inert gas to shield the weld region from atmospheric contamination.

Austenitic stainless steel SS-304 grade was selected for this study as this is the most generally utilized grade of stainless steel. The chemical composition of the SS-304 grade is given in Table 1. The test specimens were prepared with the dimensions of 100 x 150 mm with 6mm thickness. The surface of metallic plates was cleaned with 100 grit size abrasive paper to expel every surface contamination and was additionally cleaned with acetone before welding.

Active flux was prepared by mixing the SiO_2 powder with acetone in 1:1 ratio to have paint like consistency. It was applied with a paint brush on the weld surface area before welding. Acetone being a volatile liquid evaporates leaving behind a layer of SiO_2 powder stuck with the base metal.

TABLE 1. Chemical Composition of SS-304

Element	C	Cr	Ni	P	S
Age,%	0.069	18.8	8.02	0.0341	0.0103
Element	Si	Mo	Cu	Mn	Fe
Age, %	0.312	0.242	0.434	0.985	Balance

Autogenous bead on plate welds was performed in a single pass at 180 A welding current and 2mm/s welding speed keeping all welding variables identical. To evaluate mechanical properties of the joint, two plates of size 100x150x6 mm were welded with a square butt joint with the same welding parameters as that of autogenous welds on both sides to ensure complete penetration of the weld.

After welding, the weld samples were sectioned in the transverse direction and specimens for metallographic testing were prepared by grinding and polishing the specimen. Etching was done by dipping the specimen in a solution of HCl, $CuSO_4$ and distilled water. The weld bead cross-sections were photographed by Leica Microscope at different magnifications. Microhardness of the specimens was evaluated by Vickers hardness testing machine. A high-speed camera was used to capture the image of arc column amid welding. Tensile tests were performed on DAK Series 7200 UTM installed with a load cell of 100 kN. Impact test was performed on Hieco's Impact testing machine. Fractography of tensile samples was performed on JEOL Scanning Electron Microscope machine.

3. RESULTS AND DISCUSSION

3. 1. Weld Bead Geometry and Arc Column After etching, the weld bead was revealed and recorded by using an optical microscope. Weld bead measurement was done with tool maker's microscope. Figure 3 shows the weld beads obtained with and without flux at 5lpm and 15 lpm flow rate of inert gas. There was a noteworthy difference in the weld bead shape obtained with and without SiO_2 flux. Flux assisted GTA Process has shown a tremendous increment in weld bead depth (D) with a concurrent decrease in Bead width (W). The change in penetration is attributed to the inversion of Marangoni convection flow and arc constriction. Full depth penetration of 6mm has been achieved by using SiO_2 flux. Arc column images were recorded with a high-speed camera during welding as shown in Figure 4. It was noted that the arc column diameter gets reduced when welding with flux (see Table 2). The arc cone angle was measured from the images obtained and it was observed that the arc column angle reduces from 118˚ to 92˚ by using active flux during welding. This constriction of arc increases the heat flux leading to increase weld bead penetration.

3. 2. Microstructure Figure 5 exhibits the microstructure of three zones obtained after welding i.e. Weld metal, HAZ and Base Metal. The weld metal zone depicts the formation of skeletal ferrite and lathy ferrite formation in austenite microstructure resulting from primary ferrite solidification [19, 20]. All the welded samples had shown a similar formation of ferrite after solidification of the weld metal as shown in Figure 6. The area adjacent to weld metal is largely affected by heat and is termed as heat affected zone. The temperature in the HAZ reaching above recrystallization temperature prompts the formation of new grains. The quick solidification of metal leads to the formation of larger sized grains in HAZ. Unaffected base metal exhibits a fine grain structure as that of the unwelded specimen of austenitic stainless steel of the same grade.

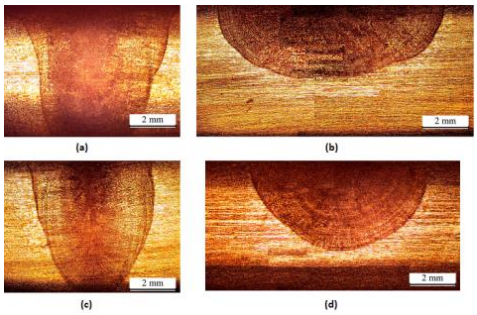

Figure 3. Weld bead macrographs for different samples as coded

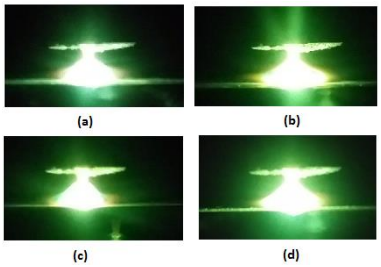

Figure 4. Arc column images for different samples as coded

TABLE 2. Experiment plan and results of bead geometry and arc column angle

Sample Code	Flux used	Gas Flow Rate (lpm)	Penetration (P) mm	Width (W) mm	Shape Factor (P/W)	Arc Column Angle (Degrees)
(a)	Yes	5	6	6.83	0.88	98^0
(b)	No	5	3.38	9.17	0.37	118^0
(c)	Yes	15	6	5.76	1.04	92^0
(d)	No	15	4.04	7.37	0.55	113^0

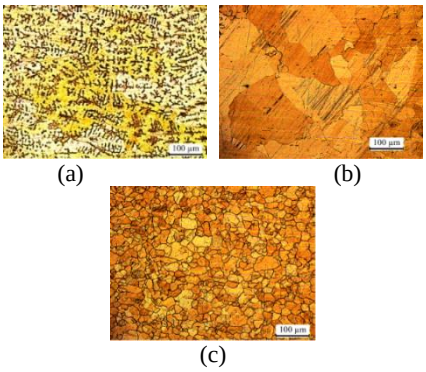

Figure 5. Microstructure of three zones, a) Weld Metal, b) HAZ, c) Base Metal

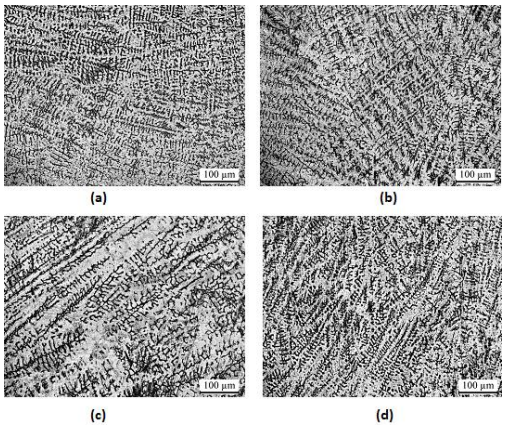

Figure 6. Microstructure at weld zone for different samples as coded

The weld metal region was investigated for the ferrite percentage in different samples. Ferrite percentage was determined by using phase expert application of Leica microscope systems. This application evaluates the ferrite content by image processing system. The dark color of skeletal ferrite and lathy ferrite is highlighted by the phase expert application and the ferrite fraction is evaluated from the total area of microstructure image. This measurement of ferrite content was evaluated at numerous positions in weld metal zone and the average ferrite content is presented in Table 3.

Results indicate 3 to 4% reduction of ferrite percentage when samples were welded with SiO_2 flux assistance. Reduction in ferrite content results from the increased solidification rates while welding with SiO_2 flux. SiO_2 flux increases the heat density by arc constriction and thus the solidification rates are also higher. At higher solidification conditions, the dendrite tip undercooling increases the stability of austenite compared to ferrite as primary phase solidification [20]. Thus, the ferrite percentage is reduced by applying Silicon dioxide flux for TIG welding of SS-304 grade stainless steel.

3. 3. Microhardness Figure 7 exhibits the micro-hardness values of weld beads prepared with different welding conditions of gas flow rate and flux application. Micro-hardness values were recorded at an interval of 250 µm and up to a distance of 8mm from weld bead center to investigate the hardness profile of the weld metal, heat affected zone and base metal.

TABLE 3. Mechanical properties of experimental samples and unwelded base metal

Sample Code	Ferrite Percentage (%)	UTS (MPa)	%age Elongation (%)	Impact Strength (J)	Microhardness at Weld Bead (HV)
(a)	24.11	634.55	41.16	289.0	177.9
(b)	27.42	678.07	46.32	285.0	180.1
(c)	24.50	651.86	42.66	297.7	178.3
(d)	28.41	671.85	44.99	263.0	181.4
Base Metal	NA	678.50	84.68	253.0	205.1

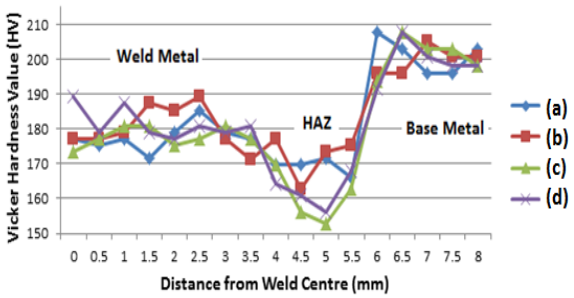

Figure 7. Microhardness profile at different welding zones

Microhardness values were evaluated by applying a load of 200 g with a dwell period of 12 seconds.

The average hardness value of weld metal in all the samples was around 180HV. HAZ has been recorded with the least hardness value with the average of 165 HV. Whereas the base metal average hardness of all the samples was 200HV. The low hardness value of HAZ zone can be ascribed to the enlarged grains formed during solidification and recrystallization of the affected metal. Average microhardness values at the weld beads were evaluated and presented in the Table 3. The samples

welded with the assistance of SiO_2 flux exhibits a slight reduction in the microhardness value as compared to samples welded without flux.

3. 4. Tensile Properties Mechanical test studies were performed on plates welded on both the sides with a square butt joint. Multiple specimens were extracted along the transverse direction of weld bead for tensile testing. The average values of the tensile properties have been reported in Table 3. Tensile tests ascertained that the failure occurs at the weld zone of almost all the samples in agreement with the microhardness values. Average microhardness values at the fusion zone were recorded lower than the average hardness values of the base metal. Further, the ferrite content of samples welded without application of flux was slightly greater than those welded with flux. Impact of ferrite content on tensile properties of austenitic stainless steel has been studied by Hauser and Van [21, 22]. Their results indicate that increment in weld metal ferrite content can enahnce the tensile strength at room temperature. The same is reflected in this study. As the ferrite content of samples welded without flux was evaluated to be greater than the samples welded with flux. The tensile strength of samples welded without flux is also greater than those welded with flux and is equivalent to that of base metal. The average values of the tensile strength of samples welded with flux exhibited a satisfactory value of 93.5 and 96% joint efficiency.

3. 5. Impact Strength Charpy tests were performed to evaluate the fracture toughness of samples. Samples for Charpy tests were prepared as per ASTM E23 standard as shown in Figure 8. Multiple specimens along the transverse direction were extracted for impact testing. The average values of impact values are reported in Table 3. V-notch was prepared in center of the weld bead to observe the fracture toughness of joint at the fusion zone. The effect of ferrite content on fracture toughness was reported by Lippold et al. [19] that fracture toughness reduces with the increase of ferrite content of weld metal. Results acquired in this study are in concurrence with the outcomes detailed by Lippold et al. [19]. Samples welded with flux exhibits lesser ferrite content and higher impact strength. The average Impact strength values of specimen welded with flux are greater than those welded without flux. The impact strength of parent metal samples was reported lower than all the welded samples. This effect may be correlated to the quick cooling of samples after welding as compared to the heat treatment given to parent material.

3. 6. Fractography Figure 9 exhibits the SEM images of fractured tensile test samples. The dimple structure obtained in SEM images articulates that the failure is ductile.

a)Tensile Samples b) Impact Samples

Figure 8. Tensile and Impact sample images before and after fracture

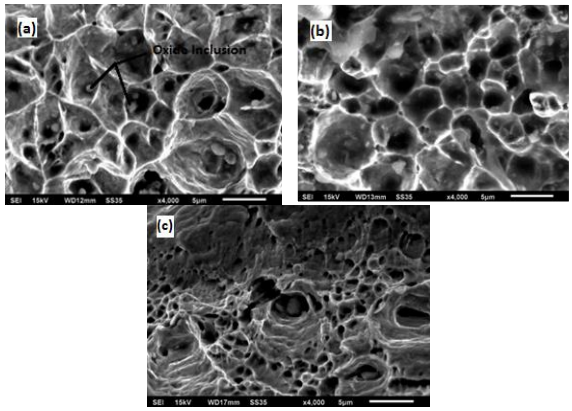

Figure 9. SEM images of fractured tensile samples (a) Welded with flux (b) Without flux (c) Unwelded base metal

The fractography image of base metal (unwelded) specimen shows the presence of dense dimple structure as compared to the fractography images of welded samples. The dense dimple structure enunciates highly ductile failure.

The tensile test outcomes are in concurrence with the fractography images obtained. The base metal specimen failure is more ductile as compared to the welded specimens and same is reflected in the UTS value and percentage elongation which are higher than the welded samples. Rapid solidification after welding reduces the ductility of metal at the fusion zone. Further, the fractography image of sample welded with SiO_2 flux reveals the presence of oxide inclusions. These oxide inclusions result from the presence of SiO_2 particles on the surface before welding. However, the sample welded without flux does not show any major oxide inclusion in he fractography images.

4. CONCLUSIONS

The experimentation study was performed to assess the effect of applying SiO_2 flux on weld bead dimensions, Microstructure, Microhardness, Ferrite content and Mechanical properties for GTA welding of 6 mm thick austenitic stainless steel grade (SS-304). The conclusions made in this experimental study are outlined as follows:

1. SiO_2 flux assistance in GTA process significantly improves the weld bead penetration. Full depth penetration welds up to 6mm can be obtained by applying SiO_2 flux prior to the welding.
2. Ferrite content at the fusion zone of samples welded with SiO_2 flux is lesser than the samples welded without flux.
3. Microhardness is least in heat affected zone owing to large grains formed in that zone. Fusion zone exhibits microhardness less than the base metal. The average microhardness value at the weld zone was slightly less for the samples welded with flux.
4. The tensile strength of samples welded with SiO_2 flux is less than the samples welded without flux as well as base metal. All the samples fractured at the fusion zone. However, a satisfactory value of 93-95% joint efficiency was achieved for samples welded with flux.
5. Fractography of tensile specimens reveals the presence of oxide inclusions in the samples welded with flux. It also depicts the reduction in ductility of the welded samples as compared to unwelded base metal.
6. The impact strength of samples welded with flux is greater than the samples welded without flux.
7. Ferrite content in fusion zone controls the mechanical behavior of the welded joints. Reduction in ferrite content with the application of SiO_2 flux reduces the tensile strength and increases the impact strength of welded joints.

7. ACKNOWLEDGMENT

The authors would like to be obliged to the management of Dr. B. R. Ambedkar National Institute of Technology, Jalandhar and DAV Institute of Engineering & Technology, Jalandhar for providing laboratory facilities.

8. REFERENCES

1. Cary, H.B. and Helzer, S.C., "Modern welding technology", ***Mc Graw Hill Education***, (1979).
2. Lu, S., Fujii, H. and Nogi, K., "Marangoni convection and weld shape variations in he–co2 shielded gas tungsten arc welding on sus304 stainless steel", ***Journal of Materials Science***, Vol. 43, No. 13, (2008), 4583-4591.
3. Heiple, C., "Mechanism for minor element effect on gta fusion zone geometry", ***Welding Journal***, Vol. 61, No. 4, (1982), 97s-102s.
4. Pollard, B., "The effects of minor elements on the welding characteristics of stainless steel", ***Welding Journal***, Vol. 67, No. 9, (1988), 202s-213s.
5. Huang, H., Shyu, S., Tseng, K. and Chou, C., "Evaluation of tig flux welding on the characteristics of stainless steel", ***Science and Technology of Welding and Joining***, Vol. 10, No. 5, (2005), 566-573.
6. Modenesi, P.J., Apolinario, E.R. and Pereira, I.M., "Tig welding with single-component fluxes", ***Journal of Materials Processing Technology***, Vol. 99, No. 1-3, (2000), 260-265.
7. Tseng, K.-H., "Development and application of oxide-based flux powder for tungsten inert gas welding of austenitic stainless steels", ***Powder Technology***, Vol. 233, (2013), 72-79.
8. Chern, T.-S., Tseng, K.-H. and Tsai, H.-L., "Study of the characteristics of duplex stainless steel activated tungsten inert gas welds", ***Materials & Design***, Vol. 32, No. 1, (2011), 255-263.
9. Howse, D. and Lucas, W., "Investigation into arc constriction by active fluxes for tungsten inert gas welding", ***Science and Technology of Welding and Joining***, Vol. 5, No. 3, (2000), 189-193.
10. SINGH, G., "Selection and mechanism of using active gas in gtaw process–a review", ***Journal of Material & Metallurgical Engineering***, Vol. 8, No. 1, (2018), 49-61.
11. Thomson, J., "Xlii. On certain curious motions observable at the surfaces of wine and other alcoholic liquors", ***The London, Edinburgh, and Dublin Philosophical Magazine and Journal of Science***, Vol. 10, No. 67, (1855), 330-333.
12. Limmaneevichitr, C. and Kou, S., "Visualization of marangoni convection in simulated weld pools containing a surface-active agent", ***Welding Journal***, Vol. 79, No. 11, (2000), 324s-330s.
13. Shanping, L., Hidetoshi, F. and Kiyoshi, N., "Effects of co2 shielding gas additions and welding speed on gta weld shape", ***Journal of Materials Science***, Vol. 40, No. 9-10, (2005), 2481-2485.
14. Choudhary, S. and Duhan, R., "Effect of activated flux on properties of ss 304 using tig welding", ***International Journal of Engineering, Transactions B: Applications***, Vol. 28, No. 2, (2015), 290-295.
15. Modenesi, P.J., Colen Neto, P., Roberto Apolinário, E. and Batista Dias, K., "Effect of flux density and the presence of additives in atig welding of austenitic stainless steel", ***Welding International***, Vol. 29, No. 6, (2015), 425-432.
16. Cai, Y., Luo, Z., Huang, Z. and Zeng, Y., "Effect of cerium oxide flux on active flux tig welding of 800 mpa super steel", ***Journal of Materials Processing Technology***, Vol. 230, (2016), 80-87.
17. Tathgir, S., Bhattacharya, A. and Bera, T.K., "Influence of current and shielding gas in tio2 flux activated tig welding on different graded steels", ***Materials and Manufacturing Processes***, Vol. 30, No. 9, (2015), 1115-1123.
18. Tseng, K.-H. and Chen, K.-L., "Comparisons between TiO_2-and SiO_2-flux assisted tig welding processes", ***Journal of Nanoscience and Nanotechnology***, Vol. 12, No. 8, (2012), 6359-6367.
19. Kotecki, D. and Lippold, J., "Welding metallurgy and weldability of stainless steels", ***Wiley, Hoboken, NJ Barbero B, Ureta E (2011) Comparative study of different digitization techniques and their accuracy. Comput Aided Des***, Vol. 43, (2005), 188-206.
20. Rizvi, S.A. and Tewari, S., "Effect of different welding parameters on the mechanical and microstructural properties of stainless steel 304h welded joints", ***International Journal of Engineering, Transactions A: Basics***, Vol. 31, No. 8, (2017).
21. Hauser, D. and Vanecho, J., "Effects of ferrite content in austenitic stainless steel welds", ***Weld. J. (Miami); (United States)***, Vol. 61, No. 2, (1982).
22. Doniavi, A., Hosseini, A. and Ranjbary, G., "Prediction and optimization of mechanical properties of st52 in gas metal arc weld using response surface methodology and anova", ***International Journal of Engineering Transactions C: Aspects***, Vol. 29, No. 9, (2016), 1307-1313.

Structure-property Interaction in Flux Assisted Tungsten Inert Gas Welding of Austenitic Stainless Steel

RESEARCH NOTE

G. Singh, D. Kumar Shukla

Department of Mechanical Engineering, Dr. B.R. Ambedkar National Institute of Technology, Jalandhar, Punjab, India

P A P E R I N F O

Paper history:
Received 11 May 2018
Received in revised form 03 Januray 2019
Accepted 03 Januray 2019

Keywords:
Active Tungsten Inert Gas
Marangoni Convection
Mechanical Properties
Austenitic Stainless Steel

چکیده

فولاد ضد زنگ فولاد Austenitic فولاد SS304 با استفاده از ریز شویی ساخته شده از پودر SiO_2 و استون، با روش جوش TIG فعال جوش داده شده است. کاربرد Flux SiO_2 باعث افزایش عمق دانه جوشکاری با کاهش همزمان در عرض ورق جوش می شود. بهبود نفوذ در اثر انقباض قوس و انحراف کانال مارنگونی است. مطالعات تجربی نشان داد که جوش SiO_2 به جوشکاری TIG کمک می کند تا نفوذ باند جوشکاری بیش از ۱۰۰٪ افزایش یابد. جوش های عمیق عمیق تا ٦ میلی متر با استفاده از شار SiO_2 به دست آمد. ریزساختار با کاهش شار SiO_2 کاهش فریت در منطقه همجوشی را نشان می دهد. نمونه هایی که با شار جوش داده می شوند باعث کاهش مقاومت کششی و بهبود مقاومت ضربه می شوند. فراکتوگرافی نمونه های آزمون کششی نشان دهنده حضور اتم های اکسید در نمونه های جوش داده شده با شار است. نسبت فریت و خواص مکانیکی در مقاله ارائه شده است.

***doi**: 10.5829/ije.2019.32.01a.13*